http://dx.doi.org/10.21611/qirt.1994.039

Early detection of thermal contrast in pulsed stimulated infrared thermography

by KRAPEZ J.-C. and BALAGEAS D.

L3C, ONERA , BP 72, F-92322 CHÂTILLON-Cedex, France.

Abstract

Pulsed stimulated infrared thermography is a powerful technique for the detection of thermally resistive defects in materials. Time-resolved analysis of the surface temperature field can then be used for the identification of the defect characteristics (mainly its depth, its lateral size and its thermal resistance). Several such inversion procedures were proposed in the past. They are based either on a 1-D or on a 2-to-3D modelling of thermal transfer in the inspected material. In this paper we describe a new 1-D procedure for the defect geometry characterization (depth and lateral size). Compared to previous 1-D methods, it is less sensitive to lateral diffusion. It however retains their high speed.

Nomenclature

a_r, a_z	in-plane and axial diffusivities of the sample ($m^2 \cdot s^{-1}$)
$Cr = 100(1-T/T_{ref})$	relative contrast (%)
$CrI = T_{ref}/T$	inverted relative contrast
d	lateral size of the defect and its reduced counterpart: $d^* = d/l_1(a_z/a_r)^{1/2}$
k_z	axial conductivity ($W \cdot m^{-1} \cdot K^{-1}$)
l, l_1,	sample thickness and defect depth (m)
$l_2 = l-l_1$	back-layer thickness and its reduced counterpart: $l_2^* = l_2/l_1$
p	Laplace variable (1/s) $\quad q = (p/a_z)^{1/2}$
R	defect's resistance ($W^{-1} \cdot m^2 \cdot K$), and its reduced counterpart $R^* = Rk_z/l_1$
t	time (s), and Fourier number { $Fo = a_z t/l^2$ }; Fo^* is expressed relatively to l_1
t_{Cr}	time (s) at which a relative contrast of value Cr is detected
T, T_{ref}	front face temperature over a defect and over a defect-free region (K)

1. Introduction

Stimulated infrared thermography is now a rather well-established non-contact full-field non-destructive technique. It progressively grows from a non-destructive testing procedure to a non-destructive characterization tool. The objective is to eventually obtain a precise description of the defect characteristics from the temporal evolution of the temperature contrast field. Several inversion procedures for the defect parameters recovery were proposed during the last ten years as described in a recent review [1].

Our purpose was to define a defect identification method suited for multi-delaminations like those found in composite laminates when they were submitted to a strong enough impact. Such defects appear as delaminations located between several couple of plies. Their shape varies with depth and their size often increases from front face to rear face. Users of such composite materials are anxious, first to detect such anomalies (internal damage can be severe without, sometimes, any sign on the external impacted face), and then to evaluate their size in order either to decide on the replacement of the damaged part, or to correctly perform the eventual repair.

*The colour plates of this article are on page **XIV** at the end of the book.*

http://dx.doi.org/10.21611/qirt.1994.039

According to the specifications of the problem and having in mind the limitations of nowadays available inversion methods, we wanted to find out a local method (each pixel of the image has to be analysed independently of its neighbours), which would provide as accurately as possible the geometrical parameters of a multi-ply defect: i.e. depth and size of the individual delaminations (actually, the delaminations thermal resistance measurement is scarcely demanded by the composite materials users, their precise determination is thus here out of scope).

The local character of the method was bound to the 1-D structure of the underlying simulation model. Our purpose was thus just to find out how to alter the classical 1-D inversion approach [2, 3] in order to reduce its inherent sensitivity to lateral diffusion. It was expected that, with such a modification, the resulting "depth-gram" of the defect will be less blurred and that the delaminations borders will be better delineated.

The aforementioned classical 1-D inversion method relies on empirical relations which were established between the defect reduced parameters on one hand and some characteristic points taken on the contrast curves on the other hand [3] (the relative contrast *Cr* and its inverted counterpart *CrI* are obtained nowadays through an improved version of the normalization described in [4]):

$$l_1 = 1.63 \sqrt{a_z\, t_{Cr_{1/2}}}\; CrI_{min}^{\left(0.643 + 0.189 \log_{10}(CrI_{min}) + 0.352 \log_{10}^2(CrI_{min})\right)} \qquad (1)$$

or:

$$l_1 = \sqrt{a_z\, t_{Cr_{max}}}\; CrI_{min}^{0.97} \qquad (2)$$

and then:

$$R = 0.0286 \frac{l_1}{k_z}\, Cr_{max}^{0.952 + 0.0362\, [\log_{10}(Cr_{max})]^2} \qquad (3)$$

(compared to those presented in [2], these relations are of more general use)

They give precise results provided that the defect is far from the back face and that it is relatively wide, but they introduce errors which are rapidly growing as the reduced lateral size of the defect gets smaller. In the case, for example, of a defect having a reduced diameter d^* of only 1 and a reduced resistance R^* of 1, the defect depth will be under-estimated by 14% with eq. 1 and by 23% with eq. 2, whereas its resistance will be under-estimated by 95% with eq. 1 joined to eq. 3. Such errors are due to the strong 3-D effects which obviously take place in this case and which weren't taken into account in the model.

2. New identification method (contrast emergence detection method)

2.1 Description of the method. Depth retrieval for a 1-D defect

Although the method will be finally applied on irregularly-shaped defects, we will describe its principle on the model of a unique infinitely extended resistance (1-D heat transfer).

It is well known [5, 6] that, in the one-side configuration of pulsed stimulated infrared thermography, temperature sensitivity to defect depth grows earlier (in absolute values) than sensitivity to resistance. It was thus recommended in [6] to identify depth from a point taken as early as possible on the contrast curve, i.e. as soon as contrast emerges out of noise. An empirical relation was then given to compute the defect depth from the time occurrence of the emergence (knowing the upper layer diffusivity). Its validity domain however wasn't defined, neither was quantitatively defined the concept of emergence.

We kept the idea of performing the relative contrast measurements as early as possible and tried to develop a precise methodology.

On figure 1 we reported the temporal evolution of the front face relative contrast for different values of the defect reduced resistance R^* (as calculated with a software for 1-D heat transfer in multi-layers [7]). The defect was assumed to be located at 1/11 of the plate thickness, i.e.

http://dx.doi.org/10.21611/qirt.1994.039

the plate, at least for short times, could be considered as semi-infinite (as we are interested in the very early evolution of the contrast, the rear face can be ignored in most cases). The curves merge at short times: a relative contrast of a few percents will be reached nearly at the same time for reduced resistance higher than 1; for lower resistances one can simply choose a lower contrast threshold.

Let us now consider the analytical expressions for the 1-D temperatures in the case of a semi-infinite material heated by a Dirac pulse. Their Laplace transforms are (after a normalization by input energy and material conductivity):

$$\begin{cases} \overline{T_{ref}} \approx q^{-1} \\ \overline{T} \approx q^{-1} \left(1 + \dfrac{2 \exp(-2 q l_1)}{1 + \dfrac{2}{R k_z q} - 2 \exp(-2 q l_1)} \right) \end{cases} \quad (4)$$

The fraction can be developed at first order for an early evolution analysis. This leads to the following expression for the relative contrast:

$$\frac{Cr}{100} \cong 2 \exp\left(-\frac{1}{Fo^*}\right) - \frac{4\sqrt{\pi Fo^*}}{R^*} \exp\left(\frac{4}{R^*}\left(1 + \frac{Fo^*}{R^*}\right)\right) \operatorname{Erfc}\left(\frac{1}{\sqrt{Fo^*}} + \frac{2\sqrt{Fo^*}}{R^*}\right) \quad (5)$$

The first term corresponds to the asymptotical behaviour for a resistance infinitely growing and describes the left limiting curve in figure 1. It will be used for what we will call the 1st order inversion:

$$l_1 = \sqrt{a_z t_{Cr} \operatorname{Ln}(200 / Cr)} \quad (6)$$

By choosing a relative contrast threshold *Cr*, and measuring the time occurrence t_{Cr} when the contrast actually reaches this value, one can infer the detected defect depth through the application of eq. 6, without any knowledge of the defect resistance.

When this simple formulae is applied to the data of the curves drawn on figure 1, the defect depth is retrieved with an error (mainly an over-estimation) as depicted on figure 2. As expected the error is higher for small values of the reduced resistance. According to our experience, the practical domain for the contrast threshold is between 1% and 10% (lower values can be reached but with specific filtering of the infrared images). When the threshold is set at 1%, the depth is evaluated through eq. 6 with a systematic error lower than 4% as soon as $R^* > 1$.

In order to better characterize low resistance defects, one could use a more precise approximation of eq. 5. By developing the *Erfc* function, one obtains:

$$Cr \cong 200 \exp\left(-\frac{1}{Fo^*}\right) \left\{1 - \frac{2 Fo^*}{R^* + 2 Fo^*}\right\} \quad (7)$$

This expression defines an implicit inversion formulation which will be called of 2nd order. The defect resistance is now present in the formulae. It should thus be evaluated independently. Actually eq. 3 and eq. 7 could be used together in an iterative process for a global inversion.

We reported on figure 3 the error on defect depth as obtained by using eq. 7 and assuming that the true value of R^* is known. Improvement was obtained for all resistance values, at least for contrast thresholds ranging from ~1% to $Cr_{1/2}$. These encouraging results however conceal the difficulty to correctly evaluate depth from eq. 7 when R^* is under-estimated. As

http://dx.doi.org/10.21611/qirt.1994.039

previously mentioned this unavoidably occurs when lateral diffusion is present. An other remedy than this 2nd order inversion is therefore to be found out.

By referring to figure 2, on can notice that the different curves have very similar slopes for a given contrast value. This slope is approximately (when $0.1\% < Cr < Cr_{1/2}$):

$$\alpha \cong 0.37 + 0.175 \log_{10}(\mathrm{Cr}) + 0.0526 \log_{10}^2(\mathrm{Cr}) \qquad (8)$$

This expression can be used together with the 1st order inversion (eq. 6) when applied at two close values of the contrast threshold in order to finally provide a closer estimation of the real depth value by extrapolation at nil contrast. The final error obtained with such an extrapolation is described in figure 4. One can notice that, compared to the simple 1st order inversion (figure 2), substantial improvement is obtained provided that the threshold is chosen below $Cr_{1/2}$.

We finally adopted the following variant for the extrapolation at nil contrast: from a series of 1st order inversions performed at different threshold values lower than $Cr_{1/2}$, a linear fit is computed between Cr^{α} and the obtained depth values; the final estimation for depth is simply the ordinate at the origin.

2.2 Assessment of the identification technique when applied to a 2-D defect

Recent experimental results have shown that, for highly resistive defects of limited extend, the short time slope of the absolute contrast is correlated to depth through a relation which is nearly independent of the lateral extend (at least for $d^* > 5$) [8]. This strengthened the idea that the contrast emergence detection method should also provide good results when applied on limited defects (our motivation was precisely to devise a method able to counter lateral diffusion effects!).

The performances of this method for the identification of the depth of a size-limited defect were first assessed on surface temperature field data obtained through numerical simulations (detailed description of the finite difference model used to produce the input data for the inversion can be found in [3, 9]).

Several values were considered for the reduced lateral size of the disk-shape delamination . We will present the results pertaining to the particular case of $d^* = 3$ and $R^* = 1$ (let us recall that the eventual anisotropy of the inspected material is implicitly taken into account through the use of specifically reduced parameters).

Let us first consider the performances about delamination depth retrieval when the classical one-point identifications
occurrence detection of maximum contrast or of half-rise contrast (eq. 2 or eq. 1). On figure 5 we reported the identified profiles relatively to the flat real depth profile. Both approaches lead essentially to a depth under-estimation above the defect. Away from it, a virtual resistance is detected at higher depths. Furthermore the profiles lack of any particular features (sudden slope change for example) which could help to locate the real delamination border. Let us recall that some hints were given in the past for this task. They refer to the contour at 40% or 50% of the contrast maximum, or to the contour at steepest contrast slope [3, 5, 10]. However the aforementioned rules are only valid for the case of uniform resistance delaminations.

One can add that the resistance profile inferred through the use of eq. 3 is considerably damped as compared to the real one (see figure 6): depending on which way depth is evaluated, the delamination resistance is under-estimated by 56% or 61% at the centre, and up to 80% at the border. These disappointing results nevertheless emphasized the benefit of founding depth identification on the early contrast behaviour.

Depth evaluation was then performed according to the new method. Different contrast thresholds were chosen (from 6% down to 0.5%). This time, depth was over-estimated in all cases, especially near the defect border (see figure 7). As expected the error decreased with the contrast threshold. We then performed the extrapolation at nil contrast as defined earlier

http://dx.doi.org/10.21611/qirt.1994.039

and we obtained the profile as depicted on figure 7. It differs from its real counterpart essentially by less than 2%. Erratic behaviour away from the borders is due to the fact that the width of the input profiles depends on the corresponding threshold.

With all the simulated cases, the identification at incipient contrast showed an improvement over the classical 1-D method, without increasing too much the time for inversion.

The incipient contrast method provides more precise values of depth for a size-limited resistance because it exploit contrast field characteristics met at a time when lateral diffusion didn't alter too much the thermal pattern yet. It is thus expected that, in the case of superimposed delaminations which sizes increase with depth, the staggered profile of the multi-delamination should be retrieved better with the new method.

3. Experimental results

We recently reported some results obtained with an academic Plexiglas sample containing concentric rear-face-open cavities which diameter and base depth were simultaneously increasing, with a carbon-epoxy sample containing staggered Teflon implants, and with a carbon-epoxy sample multi-delaminated by impact [11].

In this paper we will present additional results in the case of an impacted 2.1 mm carbon-epoxy sample and obtained by using either pulse stimulated infrared thermography or ultrasonics.

Figure A represents a depth image of the multiple delaminations as obtained with the thermal NDE method by applying the incipient contrast method. This image was actually obtained by superimposing the depth images resulting from front-face inspection of both faces of the sample. Compared to the image obtained with the maximum contrast method, the staggered structure of the delaminations was better depicted. Figure B is a C-scan image of the sample translated in depth as obtained with ultrasonics by the pulse-echo method in total immersion. The results in figure A and B are reasonably similar. Let us however mention that if one restricted the thermographic analysis to a front-face inspection of the impacted face of the sample alone, one would hardly detect the large pointed double delamination which lays near the rear face. With the help of words dear to thermal waves practitioners, one could say that the thermal echo coming back from the deep defect is mingled with the one coming back from the rear face, preventing thus any contrast to develop. This rear-face proximity problem is well-known and it can't be solved in a front-face experimental configuration without modifying the boundary condition at the back face (by cooling it by forced convection, for example).

4. Conclusions

Nowadays developed multi-dimensional "defectometric" inversion methods are not well suited for the characterization of complex-shaped defects like multi-delaminations yet. We thus devised a local method for defect depth and size identification which is based on the detection of the relative contrast emergence. Its version with extrapolation to nil contrast theoretically provides precise results for 1-D and 2-D single defects, whatever their resistance and lateral extend could be. Experiments have however shown that this extrapolation doesn't perform well on all the type of staggered defects that we considered. In any case, it was nevertheless found that the front envelope of the damaged region is retrieved better with the incipient contrast method than with the classical maximum contrast method. If a front-face experiment can be performed on both sides of the material, a global envelope of the damaged region can thus be built. The shapes obtained for the defects that we considered corresponded reasonably well to their real counterpart.

http://dx.doi.org/10.21611/qirt.1994.039

REFERENCES

[1] VAVILOV (V.P.), *Advances in signal inversion with applications to infrared thermography* - Advances in Signal Processing for Nondestructive Evaluation of Materials, NATO ASI Series E, vol; 262, 1994, p. 161-184.

[2] BOSCHER (D.M.), BALAGEAS (D.L.), DEOM (A.A.) and GARDETTE (G.), *Non destructive evaluation of carbon-epoxy laminates using transient infrared thermography* - 16th NDE Symposium, San Antonio (Texas), 21-23 april 1987.

[3] KRAPEZ (J.-C.), *Contribution a la caractérisation des défauts de type délaminage ou cavité par thermographie stimulée.* Doctoral Thesis, Ecole Centrale de Paris, Châtenay-Malabry (1991).

[4] KRAPEZ (J.-C.), BOSCHER (D.M.), DELPECH (Ph.), DEOM (A.A.), GARDETTE (G.), and BALAGEAS (D.L.), *Time-resolved pulsed stimulated infrared thermography applied to carbon-epoxy non destructive evaluation* , in Proc. of QIRT 92, July 7-9, 1992, Chatenay-Malabry, France, p. 195-200.

[5] MAILLET (D.), HOULBERT (A.S.), DIDIERJEAN (S.), LAMINE (A.S.), and DEGIOVANNI (A.), *Non destructive thermal evaluation of delaminations in a laminate,* Composites Science and Technology, vol. 47, p. 137-172.

[6] BONTAZ (J.), *Une méthode photothermique impulsionnelle appliquée au contrôle de matériaux composites.* Doctoral Thesis, Bordeaux University (1990).

[7] KRAPEZ (J.-C.) and CIELO (P.), *Thermographic nondestructive evaluation: data inversion procedures. Part I: 1-D analysis.* Research in Nondestructive Evaluation, 3 , 1991, p. 81-100.

[8] LAU (S.K.), ALMOND (D.P.) and MILNE (J.M.), *A quantitative analysis of pulsed video thermography.* NDT & E International, vol. 24(4), 1991, p.195-202.

[9] KRAPEZ (J.-C.), MALDAGUE (X.) and CIELO (P.), *Thermographic nondestructive evaluation: data inversion procedures. Part II: 2-D analysis and experimental results.* Research in Nondestructive Evaluation, 3 , 1991, p. 101-124.

[10] ALMOND (D.P.) and LAU (S.K.), *Defect sizing by transient thermography. I: an analytical treatment.* J. Phys. D: Appl. Phys., vol. 27, 1994, p. 1063-1069.

[11] KRAPEZ (J.-C.), BALAGEAS (D.), DEOM (A.), and LEPOUTRE (F.), *Early detection by stimulated infrared thermography. Comparison with ultrasonics and holo/shearography.* see [1], p.303-321.

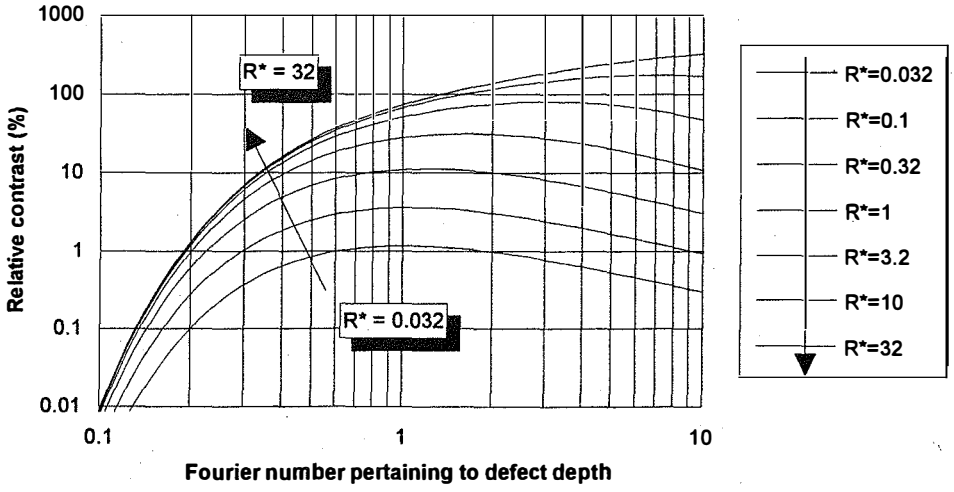

Fig.1. - Early evolution of relative contrast in 1-D transfer when I_2^*=10 (Dirac pulse, no heat losses)

http://dx.doi.org/10.21611/qirt.1994.039

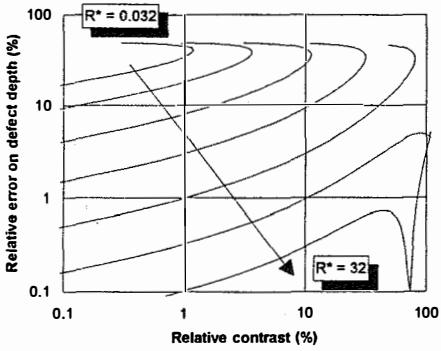

Fig.2. - Error on defect depth with 1st order inversion (input data from Fig. 1)

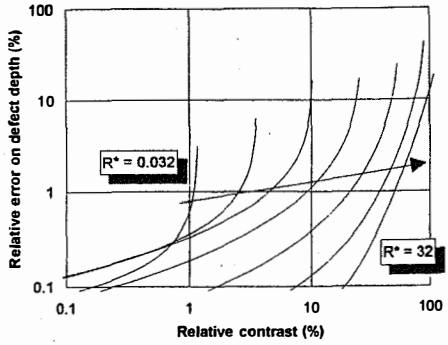

Fig.3. - Error on defect depth with 2nd order inversion (input data from Fig. 1)

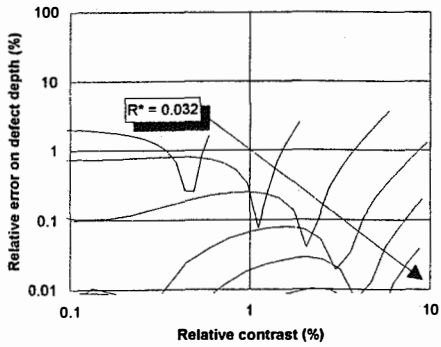

Fig.4. - Error on defect depth with 1st order inversion followed by extrapolation at nil contrast (input data from Fig. 1)

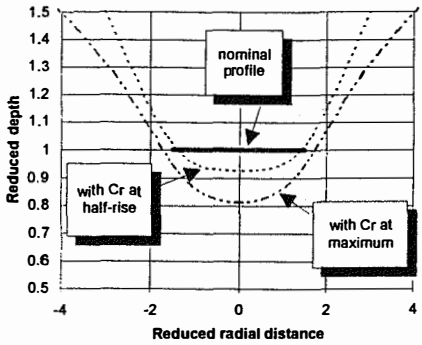

Fig.5. - Depth identification based on maximum contrast or half-rise contrast (disk-shaped delamination, d* = 3)

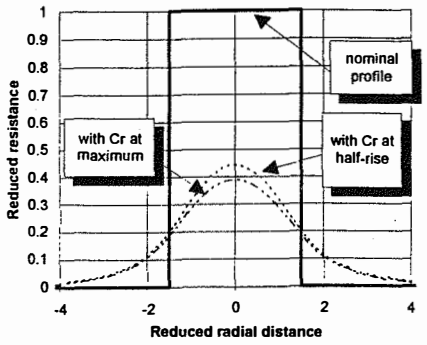

Fig.6. - Resistance identification based on maximum contrast and/or half-rise contrast occurrence (disk-shaped delamination; d* = 3)

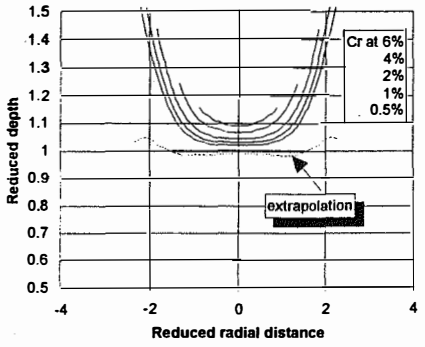

Fig.7. - As in Fig. 5 with 1st order inversion followed by extrapolation at nil contrast